

## Delocalization of a Vacancy across Two Neon Atoms Bound by the van der Waals Force

H. Sann,<sup>1</sup> C. Schober,<sup>1</sup> A. Mhamdi,<sup>2</sup> F. Trinter,<sup>1</sup> C. Müller,<sup>1</sup> S. K. Semenov,<sup>3</sup> M. Stener,<sup>4</sup> M. Waitz,<sup>1</sup>  
T. Bauer,<sup>1</sup> R. Wallauer,<sup>1</sup> C. Gohl,<sup>1</sup> J. Titze,<sup>1</sup> F. Afaneh,<sup>5</sup> L. Ph. H. Schmidt,<sup>1</sup> M. Kunitski,<sup>1</sup>  
H. Schmidt-Böcking,<sup>1</sup> Ph. V. Demekhin,<sup>2</sup> N. A. Cherepkov,<sup>3</sup> M. S. Schöffler,<sup>1</sup>  
T. Jahnke,<sup>1,\*</sup> and R. Dörner<sup>1,†</sup>

<sup>1</sup>*Institut für Kernphysik, Universität Frankfurt, Max-von-Laue-Str. 1, 60438 Frankfurt, Germany*

<sup>2</sup>*Institut für Physik und Center for Interdisciplinary Nanostructure Science and Technology, Universität Kassel,  
Heinrich-Plett-Strasse 40, 34132 Kassel, Germany*

<sup>3</sup>*State University of Aerospace Instrumentation, 190000, St. Petersburg, Russia*

<sup>4</sup>*Dipartimento di Scienze Chimiche, Università di Trieste, Via L. Giorgieri 1, I-34127 Trieste, Italy*

<sup>5</sup>*Physics Department, The Hashemite University, Zarqa 13133, Jordan*

(Received 20 April 2016; published 20 December 2016)

We experimentally study  $2p$  photoionization of neon dimers ( $\text{Ne}_2$ ) at a photon energy of  $h\nu = 36.56$  eV. By postselection of ionization events which lead to a dissociation into  $\text{Ne}^+ + \text{Ne}$  we obtain the photoelectron angular emission distribution in the molecular frame. This distribution is symmetric with respect to the direction of the charged vs neutral fragment. It shows an inverted Cohen-Fano double slit interference pattern of two spherical waves emitted coherently but with opposite phases from the two atoms of the dimer.

DOI: 10.1103/PhysRevLett.117.263001

Photoionization of homonuclear diatomic molecules has given rise to a long and controversial dispute over the seemingly clear and basic question of whether the hole created by the photoemission is located at one of the atomic centers or delocalized over both. Consequently, for the ejected electron this corresponds to the question if the photoelectron wave is emitted coherently from both sites or from either one of the two sites. The intuitive plausibility of these localization or delocalization hypotheses clearly depends on the system investigated. For valence orbitals of covalently bound molecules like  $\text{H}_2$  and  $\text{N}_2$ , obviously, a delocalized scenario seems appropriate: these orbitals create the bonds of a molecule and owe their binding to the delocalization across different atomic sites. For strongly bound inner shell electrons—and even more so for van der Waals bound systems—the answer is not that obvious.  $K$ -shell electrons, for example, are mostly located at a single atom of a molecule and van der Waals bonds rely on dipole-dipole forces and not on the sharing of electrons between atoms: a neon dimer, the system under investigation in the present study, is very similar to the case of two individual atoms and, hence, also photoionization might resemble the case of the ionization of an isolated atom. This approximate view has found apparent experimental support in previous studies [1,2].

A possible experimental observable to address the question of from which location within a diatomic molecule the photoelectron is emitted is the angular emission distribution of the photoelectron in the body-fixed frame of the molecule. Upon emission, the photoelectron wave is multiply scattered at the molecular potential and, accordingly, the emission from a single atom of the molecule can lead to an enhanced

emission towards or away from its atomic neighbor. A prominent example for this effect was observed for the case of carbon monoxide. The emission distribution of carbon  $K$ -shell photoelectrons peaks strongly in the direction of the oxygen atom for ionization energies 10 eV above the  $K$  threshold [3–7]. The same holds for Auger electrons emitted from close to the carbon center [8]. In order to observe an asymmetry of the photoelectron wave in a homonuclear diatomic molecule the two atoms of the molecule need to be distinguished. This is, for example, the case if the molecule dissociates into two ionic fragments which differ in charge. Studies of photoelectron angular distributions for such charge asymmetric breakup channels in covalently bound systems exist for the single ionization of  $\text{H}_2$  dissociating into  $p + \text{H}$  [9],  $K$ -shell ionization of  $\text{N}_2$  fragmenting into  $\text{N}^+ + \text{N}^{2+}$  [7] and  $\text{O}_2$  dissociating into  $\text{O} + \text{O}^+$  [10]. In all cases mostly symmetric angular distributions are observed; i.e., no correlation between the photoelectron emission direction and a localized emission site of the electron is found. Only at some specific photon energies as in the region of doubly excited states of  $\text{H}_2$  [9,11,12] or at threshold [13] asymmetries have been seen. In these cases, the mechanisms which create the entanglement between the bound and ejected electrons are well understood. For  $\text{Ne}_2$ , the only van der Waals system which has been studied so far, the situation is different [1,2]. Ne  $K$ -shell ionization leading to  $\text{Ne}^+ + \text{Ne}^{2+}$  showed asymmetric photoelectron and valence shell autoionization electron angular distributions without any of the before-mentioned mechanisms being active.

The way out of this inconclusive status of the discussion has been suggested by multicoincidence studies on covalently bound  $\text{N}_2$  and  $\text{O}_2$ . They proved that the notion of

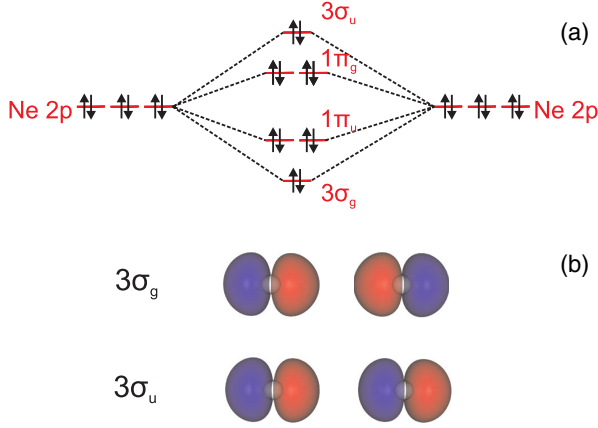


FIG. 1. (a) The molecular orbitals of the neon dimer which are formed from the  $2p$  orbitals of the two neon atoms. (b) The calculated shape of the  $3\sigma_g$  and  $3\sigma_u$  orbitals [19]. They are in very good approximation a superposition of  $2p$  orbitals located at both cores.

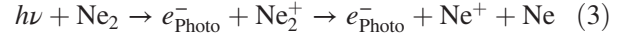
localized vs delocalized vacancies is often a misleading oversimplification [11,14–16] as it is based on a single-particle picture of the hole or the emitted electron, which is a very crude approximation. A full description of photoionization and subsequent fragmentation of the molecule, however, has to take into account that electrons and ions form an entangled few-body state in the continuum. Accordingly, signatures of apparent localized or delocalized holes can be found depending on the detection performed on the emitted fragments. The purpose of the present Letter is to further support this “full story” by showing that even for a van der Waals system for which apparent localization of a vacancy has been reported [1,2], a suitable choice of observables can also yield the opposite, namely, clear signatures of delocalization. For the  $2p$  photoionization of  $\text{Ne}_2$  leading to a breakup into  $\text{Ne}^+ + \text{Ne}$  we find evidence for a coherent emission of the electron from both atomic sites. The evidence for delocalization we find is twofold: first, the electron angular distribution is symmetric with respect to the emission directions of the  $\text{Ne}$  and  $\text{Ne}^+$  fragments and, second, we observe the typical interference pattern expected for an emission from two coherent sources, already predicted by Cohen and Fano several years ago [17].

The valence electrons of  $\text{Ne}_2$  in a localized and delocalized notation are shown in Fig. 1(a). The wave function of the dimer ion is to a very good approximation described by a linear combination of atomic orbitals of the contributing atoms. The symmetry adapted gerade and ungerade wave functions  $\varphi_{\text{Ne}_2^+}^{g,u}$  of  $\text{Ne}_2^+$  are thus given by linear combinations of the wave functions  $\varphi_{\text{Ne}^+\text{Ne}}^l$  and  $\varphi_{\text{NeNe}^+}^r$  of a  $\text{Ne}^+$  ion with a vacancy in the  $p_z$  or  $p_{xy}$  orbital and a neutral  $\text{Ne}$  atom on the left or right side:

$$\varphi_{\text{Ne}_2^+}^g = 1/\sqrt{2}(\varphi_{\text{Ne}^+\text{Ne}}^l + \varphi_{\text{NeNe}^+}^r), \quad (1)$$

$$\varphi_{\text{Ne}_2^+}^u = 1/\sqrt{2}(\varphi_{\text{Ne}^+\text{Ne}}^l - \varphi_{\text{NeNe}^+}^r). \quad (2)$$

The ground state of  $\text{Ne}_2$  is of gerade parity, the photon parity is ungerade. Thus, by parity conservation the few body wave function  $\Psi_{e,\text{Ne}_2^+}$  of the reaction products of



must be of ungerade parity. This does, however, not entail that the continuum electron wave function  $\varphi_{e_{\text{Photo}}^-}$  or the  $\text{Ne}_2^+$  wave function  $\varphi_{\text{Ne}_2^+}$  both initially have well-defined parity. It is only the Bell-type state describing all the reaction products that has a well-defined parity:

$$\Psi_{e,\text{Ne}_2^+} = 1/\sqrt{2}(\varphi_{e_{\text{Photo}}^-}^g \varphi_{\text{Ne}_2^+}^u + \varphi_{e_{\text{Photo}}^-}^u \varphi_{\text{Ne}_2^+}^g) \quad (4)$$

$$= 1/\sqrt{2}(\varphi_{e_{\text{Photo}}^-}^l \varphi_{\text{Ne}^+\text{Ne}}^l - \varphi_{e_{\text{Photo}}^-}^r \varphi_{\text{NeNe}^+}^r). \quad (5)$$

The outcome of a coincidence measurement of the constituents of such a Bell state depends on the basis onto which the measurement projects its wave function. In a coincidence measurement of polarization entangled photons (see, e.g., Ref. [18]), which is described by the same formalism, the experimentalist can freely choose the basis by simply rotating a photon polarizer in front of one detector. For photofragmentation of molecules the experimentalist is able to actually choose the desired basis only in distinct cases. An example where this has been possible is  $K$ -shell ionization of  $\text{N}_2$  where the photoelectron and Auger electron form such a Bell state [14,15]. In this case, by varying the detection angle of the Auger electron, a switching between the localized and the symmetry adapted basis is performed and the associated angular emission distribution of the photoelectron measured in coincidence is seen. In many other cases the choice of the basis is determined by the dissociation pathways, i.e., the details of the potential energy curves involved in the reaction and the transitions between them. For  $2p$  ionization of  $\text{Ne}_2$  the relevant potential energy surfaces are shown in Fig. 2. A peculiarity of these curves allows us to choose a particularly clean detection signal with which we can postselect the  $\text{Ne}_2^+$  wave function in a state of pure  $g$  symmetry: only one of the accessible potential energy curves (i.e., the  ${}^2\Sigma_g^+$  curve), is dissociative. Thus, by detecting photoionization events which lead to dissociation we postselect  $\text{Ne}_2^+$  in a gerade state and we can then examine whether the photoelectrons recorded in coincidence are of corresponding symmetry as predicted by Eq. (5).

The experiment was performed at the BESSY synchrotron radiation source at beam line UE112 PGM-1 in single bunch operation using the COLTRIMS technique to measure the momentum vectors of the photoelectron and the  $\text{Ne}^+$  fragment in coincidence [21–23]. Circularly polarized photons ( $h\nu = 36.56$  eV) were focused into a supersonic neon gas jet, creating photoelectrons of  $\approx 15$  eV kinetic energy. The gas jet was precooled to 140 K and contained roughly 2% of dimers. The electrons and ions were guided by electric and magnetic fields to two position- and time-sensitive MCP

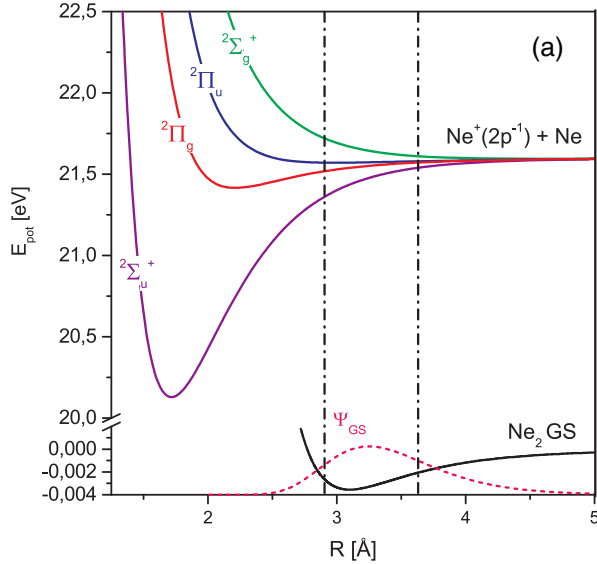


FIG. 2. Potential energy curves of the neon dimer after removal of a valence electron. For simplicity we have omitted the spin orbit interaction. Even if spin orbit splitting is taken into account, the  $\Sigma$  state with gerade parity remains the only dissociating state [20]. The ground state potential curve and wave function  $\Psi_{GS}$  of the neutral dimer is also shown.

detectors with delay line readout [24]. The electron arm of the spectrometer employed McLaren time focusing [25] and on the ion arm (with an overall length of 473 mm) an electrostatic lens was used to improve the momentum resolution [15]. More detailed information of the experimental setup are to be found in the Supplemental Material [26]. By measuring the photoelectron and the ion momenta in coincidence, the relative emission angle between the two is obtained yielding the electron emission distribution in the body-fixed frame as shown in Figs. 3(b) and 3(c).

In Fig. 3 electrons and ions are both emitted within the polarization plane of the circularly polarized light. The dimer is oriented horizontally. The electron angular distribution is highly structured but symmetric with respect to the emission direction of the  $\text{Ne}^+$  and Ne fragments. This observed symmetry is a first evidence, supporting the above analysis, that photoelectrons which are measured in coincidence with a fragmentation of the neon dimer belong to a state of well-defined parity, as an *asymmetric* angular distribution would have been a clear evidence of a superposition of gerade and ungerade states being ionized.

As a next step to check our assumption of a delocalized electron emission we test whether the photoelectron is emitted coherently from both atomic sites and whether the parity of the wave function is gerade or ungerade. We follow [17] and model the angular distribution by a coherent superposition of two spherical waves emitted from two sources spaced by an internuclear distance  $R$  [see Fig. 3(a)]. The phase shift between the two waves depends on the parity of the wave function and on the shape of the involved atomic orbitals [35],

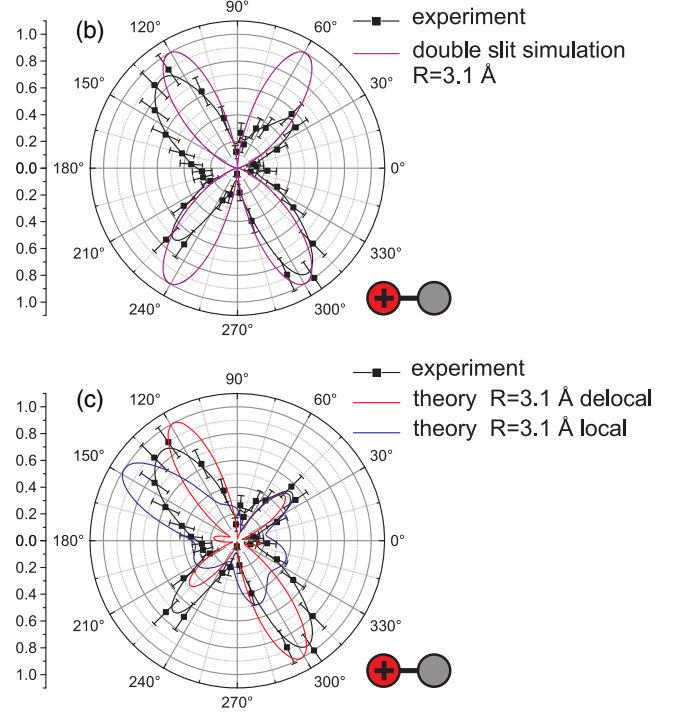
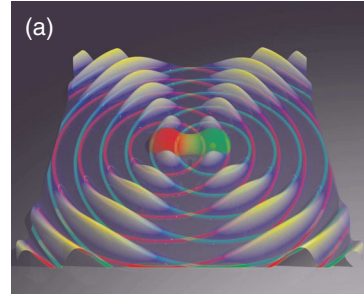


FIG. 3. (a) Graphical representation of the conducted double slit simulation. A spherical wave is emitted from each neon core. The relative phase of the waves depends on the shape of the atomic orbital from which the electrons are emitted [see Eq. (6)]. (b) The experimental molecular frame photoelectron angular distribution (black dots) is compared to the double slit simulation (purple line). The simulation was done for a fixed electron energy of 15 eV and a fixed internuclear distance of 3.1 Å. The measurement was done at a fixed photon energy of 36.56 eV. This corresponds to an electron energy of 15 eV. The experimental data is integrated over all measured internuclear distances. (c) The experimental data is compared to full quantum mechanical calculations for localized emission from the left atom (blue line) and delocalized emission (red line). The calculations were done using the following parameters:  $h\nu = 36.56$  eV and  $R = 3.1$  Å. The direction of the  $\text{Ne}^+$  ion in (b) and (c) is  $180^\circ$ .

$$\Psi(\vec{p}) = e^{i\vec{p}(\vec{R}/2)} + (-1)^{l-m+\lambda} e^{-i\vec{p}(\vec{R}/2)}, \quad (6)$$

where  $l$  and  $m$  are the orbital and magnetic quantum numbers,  $\lambda$  equals  $m$  for gerade parity, and  $m+1$  for ungerade parity. The momentum  $\vec{p}$  of the electron corresponds to the continuum wavelength ( $\lambda = h/p$ ). For  $p$  orbitals, which are arranged horizontally with respect to the molecular axis ( $m = 0$ ), and gerade parity

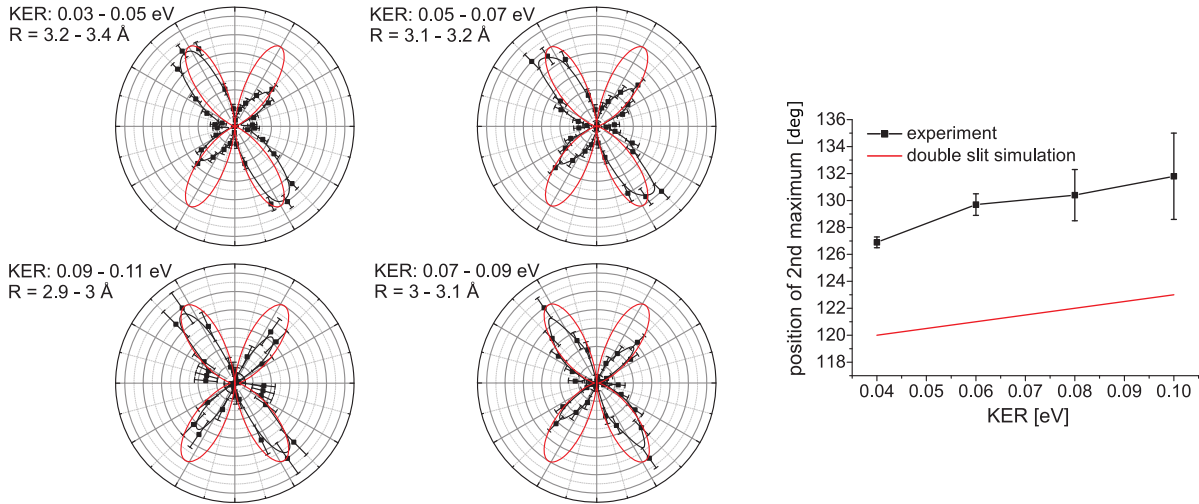


FIG. 4. Comparison of the measured MFPAD (black dots) and the double slit simulation (red lines) for different internuclear distances, respectively, different KER. The direction of the  $\text{Ne}^+$  ion is the same as in Fig. 3.

the magnitude squared of the wave function can be written as follows:

$$|\Psi|^2 = 4\sin^2\left(\vec{p} \cdot \frac{\vec{R}}{2}\right) = 4\sin^2\left(p \frac{R}{2} \cos\theta\right); \quad (7)$$

$\theta$  is the angle relative to the molecular axis and, therefore,  $|\Psi|^2$  can be directly compared to the measured and normalized angular distribution [Fig. 3(b)]. This simple double slit simulation already accounts for the four-lobe structure we observe in the experiment. The nodal feature at  $90^\circ$ , furthermore, unveils the parity of the state directly. Comparing the measured distribution and the simple model in more detail shows that the positions of the maxima differ slightly and, furthermore, the simulation cannot reproduce the different sizes of the maxima obtained from the experiment. This is obviously due to oversimplification of our double slit model: the simulation does, for example, not take into account the interaction of the departing electron with the molecular potential; i.e., it neglects any scattering of the electron at the other atom.

To factor in these effects into a delocalized scenario we performed a full quantum mechanical calculation which was carried out by the single center method and code [36,37]. More information on the theory can be found in the Supplemental Material [26]. The corresponding results of these calculation are shown in Fig. 3(c) by the red solid line. The main features observed in the experiment are now reproduced: we observe a point-symmetric four-lobe structure with two of the lobes being substantially larger than the other two.

In order to further support our conclusion of a delocalized coherent emission from both sides, we show the quantum mechanical prediction for the opposite case, i.e., for a localized emission from only one center, as well, in Fig. 3(c). The effect of localization is created in the calculation by a coherent superposition of emission from

the orbitals  $3\sigma_g$  and  $3\sigma_u$ . As one can see from the graph, a localized emission would indeed result in a noticeable asymmetry in the molecular frame photoelectron angular distribution (MFPAD), which is in clear disagreement with the experimental data. The data are in fair agreement with the calculation for delocalized emission with the size and position of the maxima not being completely correct. This can be explained by the fact that the theoretical distribution has been calculated for a fixed internuclear distance of  $3.1 \text{ \AA}$ , which is the equilibrium distance of the neon dimer [38], while the experimental data is integrated over all occurring internuclear distances. The position and size of the maxima is very sensitive to this parameter [39]: as one can see from Eq. (7), the simple double slit simulation already predicts the correlation between the position of maxima and  $R$ . A change in the internuclear distance results in a shift of relative phase between the electron waves emitted from the cores and, therefore, the angles under which constructive and destructive interference occurs change.

To even further support the delocalized scenario we present the experimental evidence for this subtle prediction of the  $R$  dependence [Eq. (7)] of the double slit interference in Fig. 4. The figure shows the measured MFPAD together with the double slit simulation for different  $R$ . The experimental  $R$  can be obtained from the measured kinetic energy release (KER) of the atomic fragments by using the reflection approximation [40] with the potentials shown in Fig. 1. Notably, the simulation describes the trend of the maxima of the lobes with  $R$  observed in the experiment. This further supports the assumption that the investigated process can be qualitatively described as a molecular double slit and thus supports the delocalized scenario although the scattering of the escaping electron cannot be neglected.

In summary, we have provided conclusive evidence that also for the van der Waals dimer  $\text{Ne}_2$ —a system where no electrons are shared among the extremely weakly bound atoms—a proper postselection of photoelectrons yields

electron angular distributions which are of well-defined parity. This postselection can be achieved for  $2p$  ionization by detecting the fragmentation of the  $\text{Ne}_2^+$  into  $\text{Ne}^+ + \text{Ne}$ . The electron angular distribution is thus symmetric with respect to the direction to which the charged fragment is emitted. Furthermore, the angular distribution shows an interference structure expected for coherent emission from both sides and even the corresponding dependence on the internuclear distance. This postselection was possible because  $^2\Sigma_g^+$  is the only dissociating  $\text{NeNe}^+$  state after  $2p$  ionization. In a previous  $\text{Ne}_2$   $K$ -shell ionization experiment [1] the sequence of photoionization followed by Auger decay and interatomic Coulombic decay leading to  $\text{NeNe}^{3+}$  yields to a coherent population of gerade and ungerade  $\text{NeNe}^{3+}$  states. The detection of the  $\text{Ne}^{2+}$  then leads to the correlated detection of a photoelectron belonging to a localized hole. We conclude that the picture of localization or delocalization of a single particle or hole in this many-body wave function is oversimplified and quantum mechanically ill posed. In coincidence experiments on molecular ionization one has to carefully discuss what is actually measured and to which basis set this measurement projects the few-body wave function just as in any coincidence measurement on entangled photons.

We want to thank the staff of BESSY II for experimental support. This work was funded by DFG.

\*jahnke@atom.uni-frankfurt.de

†doerner@atom.uni-frankfurt.de

- [1] K. Kreidi *et al.*, *J. Phys. B: At., Mol. Opt. Phys.* **41**, 101002 (2008).
- [2] M. Yamazaki, J. I. Adachi, Y. Kimura, A. Yagishita, M. Stener, P. Decleva, N. Kosugi, H. Iwayama, K. Nagaya, and M. Yao, *Phys. Rev. Lett.* **101**, 043004 (2008).
- [3] F. Heiser, O. Geßner, J. Viehhaus, K. Wieliczek, R. Hentges, and U. Becker, *Phys. Rev. Lett.* **79**, 2435 (1997).
- [4] B. Zimmermann *et al.*, *Nat. Phys.* **4**, 649 (2008).
- [5] N. A. Cherepkov, G. Raseev, J. Adachi, Y. Hikosaka, K. Ito, S. Motoki, M. Sano, K. Soejima, and A. Yagishita, *J. Phys. B: At., Mol. Opt. Phys.* **33**, 4213 (2000).
- [6] A. Landers *et al.*, *Phys. Rev. Lett.* **87**, 013002 (2001).
- [7] T. Weber *et al.*, *J. Phys. B* **34**, 3669 (2001).
- [8] T. Weber *et al.*, *Phys. Rev. Lett.* **90**, 153003 (2003).
- [9] A. Lafosse, M. Lebech, J. C. Brenot, P. M. Guyon, L. Spielberger, O. Jagutzki, J. C. Houver, and D. Dowek, *J. Phys. B: At., Mol. Opt. Phys.* **36**, 4683 (2003).
- [10] A. V. Golovin, F. Heiser, C. J. K. Quayle, P. Morin, M. Simon, O. Gessner, P. M. Guyon, and U. Becker, *Phys. Rev. Lett.* **79**, 4554 (1997).
- [11] F. Martin *et al.*, *Science* **315**, 629 (2007).
- [12] D. Dowek, J. F. Pérez-Torres, Y. J. Picard, P. Billaud, C. Elkharrat, J. C. Houver, J. L. Sanz-Vicario, and F. Martin, *Phys. Rev. Lett.* **104**, 233003 (2010).
- [13] V. V. Serov and A. S. Kheifets, *Phys. Rev. A* **89**, 031402 (2014).
- [14] M. S. Schöffler *et al.*, *Science* **320**, 920 (2008).
- [15] M. S. Schöffler *et al.*, *New J. Phys.* **13**, 095013 (2011).
- [16] X.-J. Liu, Q. Miao, F. Gel'mukhanov, M. Patanen, O. Travnikova, C. Nicolas, H. Agren, K. Ueda, and C. Miron, *Nat. Photonics* **9**, 120 (2015).
- [17] H. Cohen and U. Fano, *Phys. Rev.* **150**, 30 (1966).
- [18] S. Freedman and J. Clauser, *Phys. Rev. Lett.* **28**, 938 (1972).
- [19] M. J. Frisch *et al.*, *Gaussian 03, Revision C.02* (Gaussian, Inc., Wallingford, 2004).
- [20] J. S. Cohen, *J. Chem. Phys.* **61**, 3230 (1974).
- [21] R. Dörner, V. Mergel, O. Jagutzki, L. Spielberger, J. Ullrich, R. Moshhammer, and H. Schmidt-Böcking, *Phys. Rep.* **330**, 95 (2000).
- [22] J. Ullrich, R. Moshhammer, A. Dorn, R. Dörner, L. P. Schmidt, and H. Schmidt-Böcking, *Rep. Prog. Phys.* **66**, 1463 (2003).
- [23] T. Jahnke, T. Weber, T. Osipov, A. Landers, O. Jagutzki, L. Schmidt, C. Cocke, M. Prior, H. Schmidt-Böcking, and R. Dörner, *J. Electron Spectrosc. Relat. Phenom.* **141**, 229 (2004).
- [24] O. Jagutzki, A. Cerezo, A. Czasch, R. Dörner, M. Hattas, V. Mergel, U. Spillmann, K. Ullmann-Pfleger, T. Weber, H. Schmidt-Böcking, and G. Smith, *IEEE Trans. Nucl. Sci.* **49**, 2477 (2002).
- [25] W. C. Wiley and I. H. McLaren, *Rev. Sci. Instrum.* **26**, 1150 (1955).
- [26] See Supplemental Material at <http://link.aps.org/supplemental/10.1103/PhysRevLett.117.263001> for brief description of the experimental and theoretical methods, which includes Refs. [27–34].
- [27] R. Moshhammer *et al.*, *Phys. Rev. Lett.* **73**, 3371 (1994).
- [28] R. Moshhammer, M. Unverzagt, W. Schmitt, J. Ullrich, and H. Schmidt-Böcking, *Nucl. Instrum. Methods Phys. Res., Sect. B* **108**, 425 (1996).
- [29] D. R. Miller, *Atomic and Molecular Beam Methods* (Oxford University Press, Oxford, 1988).
- [30] Ph. V. Demekhin, I. D. Petrov, V. L. Sukhorukov, W. Kielich, P. Reiss, R. Hentges, I. Haar, H. Schmoranzer, and A. Ehresmann, *Phys. Rev. A* **80**, 063425 (2009); **81**, 069902(E) (2010).
- [31] Ph. V. Demekhin, I. D. Petrov, V. L. Sukhorukov, W. Kielich, A. Knie, H. Schmoranzer, and A. Ehresmann, *Phys. Rev. Lett.* **104**, 243001 (2010).
- [32] Ph. V. Demekhin, I. D. Petrov, V. L. Sukhorukov, W. Kielich, A. Knie, H. Schmoranzer, and A. Ehresmann, *J. Phys. B* **43**, 165103 (2010).
- [33] D. Woon and J. T. H. Dunning, *J. Chem. Phys.* **100**, 2975 (1994).
- [34] T. Jahnke *et al.*, *Phys. Rev. Lett.* **88**, 073002 (2002).
- [35] X. Lai and C. F. d. M. Faria, *Phys. Rev. A* **88**, 013406 (2013).
- [36] P. V. Demekhin, A. Ehresmann, and V. L. Sukhorukov, *J. Chem. Phys.* **134**, 024113 (2011).
- [37] S. A. Galitskiy, A. N. Artemyev, K. Jänkälä, B. M. Lagutin, and P. V. Demekhin, *J. Chem. Phys.* **142**, 034306 (2015).
- [38] F.-M. Tao and Y.-K. Pan, *Chem. Phys. Lett.* **194**, 162 (1992).
- [39] M. S. Schöffler *et al.*, *Phys. Rev. A* **78**, 013414 (2008).
- [40] H. D. Hagstrum, *Rev. Mod. Phys.* **23**, 185 (1951).